

Nonequilibrium Effects of Anisotropic Compression Applied to Vortex Lattices in Bose-Einstein Condensates

P. Engels, I. Coddington, P. C. Haljan, and E. A. Cornell*
*JILA, National Institute of Standards and Technology and Department of Physics,
University of Colorado, Boulder, Colorado 80309-0440*

(February 1, 2008)

We have studied the dynamics of large vortex lattices in a dilute-gas Bose-Einstein condensate. While undisturbed lattices have a regular hexagonal structure, large-amplitude quadrupolar shape oscillations of the condensate are shown to induce a wealth of nonequilibrium lattice dynamics. When exciting an $m = -2$ mode, we observe shifting of lattice planes, changes of lattice structure, and sheet-like structures in which individual vortices appear to have merged. Excitation of an $m = +2$ mode dissolves the regular lattice, leading to randomly arranged but still strictly parallel vortex lines.

03.75.Fi,67.90.+z,67.40.Vs,32.80.Pj

The experimental study of vorticity in a dilute-gas Bose-Einstein condensate (BEC) provides an useful perspective on superfluidity. While the focus of early work was on the study of single or few vortices [1,2], recent advances in technique have made it possible to create BECs containing large amounts of vorticity [3–6]. In a rapidly rotating BEC, a lattice of vortices is the lowest energy state in the rotating frame [7]. Experimental studies of lattices to date have concentrated on formation and decay processes [2–6,8,9]. In this Letter we study the nonequilibrium behavior of vortex lattices under large-amplitude, anisotropic strain.

Experimental technique For creating large amounts of vorticity in condensates, we use a modified version of the spin-up technique described in our previous paper [5]. The starting point is a magnetically trapped cloud of 17×10^6 ^{87}Rb atoms in the $|F = 1, m_F = -1\rangle$ state with a temperature approximately three times above the critical temperature for the BEC phase transition, $T_c = 67$ nK. By manipulating the ellipticity of the confining potential, we can resonantly pump angular momentum into the as yet uncondensed cloud [10]. We then tune the trapping potential to near perfect axial symmetry with trap frequencies $\{\omega_\rho, \omega_z\} = 2\pi\{8.35, 5.45\}$ Hz. In this round trap the cloud continues to rotate, and by performing a nearly one-dimensional evaporation along the axis of rotation (z-axis) as described in Ref. [5], we cool down and further spin up the cloud until a highly rotating condensate is born out of the rotating normal cloud. For the experiments described in this paper, the evaporation is continued to a point where little or no thermal fraction remains. As a result of this procedure, we obtain highly rotating condensates with typically 1×10^6 atoms, containing 130 vortices or more.

To study these condensates we can image along the x, y, or z directions. When the condensate is held in the trap, the core size of the vortices is close to the resolution limit of our optical detection system so that individual

vortices are not resolved by in-trap imaging. However, by nondestructively imaging a trapped condensate from the side (along the x-direction) and measuring its aspect ratio, the rotation rate of the condensate can be determined [5,8]. For our highly rotating condensates we determine typical aspect ratios of 0.5, which is markedly different from the static aspect ratio of the magnetic trap, 1.53, because of centrifugal forces. Typical condensate rotation rates of $0.95\omega_\rho$ are inferred.

To resolve individual vortices, we can release a condensate from the trap and image it after it has expanded by a factor of 5 [2,12]. Such expansion pictures taken along the z-direction reveal a hexagonal lattice of vortex cores in highly rotating condensates [Fig. 1(a)]. The lattice structure is remarkably regular even at the outer regions of the condensate, and is observed with very good contrast as shown by the cross section in Fig. 1(b).

When looking at such vortex lattices in expansion from the side (i.e., along the x or y direction), good contrast is only obtained if the lattice is oriented in such a way that vortices line up behind each other along the direction of view, or in other words when the direction of view is parallel to lattice planes. The vortex lattices are not stationary in the lab frame, but are rotating with the condensate, and furthermore the initial orientation of the lattice in the xy plane cannot be controlled in current experiments. Therefore the times when vortices line up along the direction of sight are unpredictable, and images revealing lattice planes are only obtained in a random subset of all trials. One example is shown in Fig. 1(c), where the vortex planes are clearly visible as dark vertical lines. These images are direct verifications of the theoretical prediction that vortex lines are only marginally bent for our experimental parameters [13,14], as is also confirmed by the good contrast seen in the topview picture of Fig. 1(a).

Vortex lattices such as the one shown in Fig. 1 are the starting point for our studies of the effects of dynamical

cally generated strain. We apply the distortion by resonantly driving quadrupolar shape modes in the vortex-filled condensate [15,16]. In the large-amplitude limit, the $m_z = +2$ and $m_z = -2$ modes distort the circular cross-section of the condensate into an ellipse and cause the major axis of the ellipse to rotate along with, or against, the sense of the condensate rotation, respectively. The generated strain is considerable – the ratio of major to minor axis of the condensate can be larger than three to one. The frequencies of the $m_z = \pm 2$ modes may be calculated using the sum rule argument given by Refs. [17,18]. Our condensates are rotating typically at $0.95\omega_\rho$, just 5% under the centrifugal limit. At the centrifugal limit, the major axis of the $m_z = +2$ ellipse is fixed in the rotating condensate frame, and the $m_z = -2$ shape is fixed in the lab frame. At our rotation rate of $0.95\omega_\rho$, the distortion, as seen in the frame of the lattice, rotates at only 0.4 Hz for the $m_z = +2$ mode, compared with 8.34 Hz for the $m_z = -2$ mode. For this reason [19], we expect very different resulting lattice dynamics in the presence of either of the two modes.

Lattice dynamics in the presence of an $m_z = -2$ surface mode Because the $m_z = -2$ mode is almost stationary in the lab frame for the parameters of our experiment, this mode can be excited conveniently and nearly resonantly by a static trap deformation. Indeed we observe that by jumping from a round trap to a trap that has an ellipticity of 3.6% [20], the ellipticity of the condensate increases over a timescale of 300 ms from approximately 0 to 40%, thereby exceeding the trap ellipticity by more than an order of magnitude. Since the vortex lattice is rotating quickly with respect to this almost static deformation, it is an interesting and nontrivial question to ask whether or not a lattice structure is maintained, and, if so, how it rearranges in the presence of the excitation.

Experimentally, vortex lattices can indeed be observed in expansion images up to 400 ms after the start of the continuously applied trap deformation (Fig. 2). Subsequently, long range order is lost and vortex visibility becomes low, presumably due to tilting [16] or bending of the vortex lines [4]. A closer look at the first 400 ms of this evolution reveals a wealth of intriguing vortex dynamics. As the vortex lattice rotates in the deformed condensate, the lattice planes must continuously shift relative to each other to accommodate to the elliptical shape of the condensate. One consequence of this is transient changes of the lattice structure. In Fig. 3 the lattice has changed from the hexagonal structure of an undisturbed lattice to a near orthorhombic structure.

The most striking observation, however, is of condensates containing sheet-like structures rather than individual vortex cores, as shown in Fig. 4(a). We interpret these sheets as rows of vorticity along which individual vortex cores have essentially merged. Given the near perfect contrast of these sheets, as shown by the cross section in

Fig. 4(b), we can exclude the possibility that the sheets are merely formed by a collective tilting of vortices along a lattice plane, which would result in an intermediate contrast. Similarly, we can rule out that this is an effect merely of imaging resolution - had the vortices retained their original structure but come so close together that we could not spatially resolve them, we again would see white stripes set off by grey troughs, rather than the near 100% alternating stripes of white and black. If there continue to exist wispy fingers of condensate that cross the stripes and differentiate individual vortices, they must be very tenuous indeed to be consistent with the observed contrast. The clouds have been continuously distorted from their original hexagonal symmetry, so the observation of 16 stripes along the major axis of the BEC in Fig. 4(a) tells us that there must also be the equivalent of 16 units of vorticity along the length of the stripes through the center of the cloud. By measuring the in-trap height of the condensate, the ellipticity in the xy-plane and the number of atoms, we can infer the ratio of unit vorticity spacing (along the minor axis) to healing length (given by $\frac{1}{\sqrt{8\pi n a}}$, where n is the mean density and a the scattering length) to be on the order of 5.

In fact the contrast of this sheet-like phase is so deep that the structure can be detected by looking at condensates *in trap* (along the x or z direction), even though the structure is close to our optical resolution limit. By taking a time series of ten nondestructive images of a single condensate along the x direction, we see that the sheet structure appears and disappears periodically with a period of about 21.2 ms for a condensate rotating at a frequency of $0.95\omega_\rho$ [Fig. 5].

This periodicity can be understood as follows: The sheet structure forms when a lattice vector lies along a minor axis of the cloud, presumably since this is when the vortices are closest together. As that vector rotates past the minor axis, structure along the vector is reestablished, the two-dimensional (2D) pattern of individual vortices reemerges, and the high-contrast stripes disappear from the in-trap images. A lattice vector aligns with the minor axis six times per lattice rotation period due to the sixfold symmetry of the unperturbed lattice, consistent with the observed frequency of periodic stripe formation. This interpretation is bolstered by the expansion images, which show high contrast sheets when a lattice vector lies close to the minor axis, but 2D lattices (albeit distorted) for other orientations. We find it remarkable that this lattice-to-sheet-to-lattice sequence persists through multiple cycles before long range order and visibility are compromised.

Using a trap with a stronger distortion of 34% as in Fig. 4(c-e), we also observe sheets breaking apart in the center. In Fig. 4(c), the density distribution along the lattice vector that we see near-parallel with the minor axis is nearly featureless. Figure 4(d,e) hint at the succeeding

lattice evolution: Fig. 4(d) represents a small rotation from Fig. 4(c), and we see that the sheets have begun to reconnect across the cloud. Figure 4(e) appears to be a continuation of that process, with considerable evidence of uniformity in the repeating structure.

Lattice dynamics in the presence of an $m_z = +2$ surface mode We excite the $m_z = +2$ mode by elliptically deforming the magnetic trap and rotating that ellipse around in the xy plane. When the $m_z = +2$ mode is driven approximately 1 Hz away from its resonance, the ellipticity of the condensate increases from 0 to 50% over a timescale of 250 msec. Under the influence of an on-resonant drive, the ellipticity increases continuously, even passing beyond 90% after 700 msec and approaching 100% [21]. As discussed above, the distortion rotates only very slowly with respect to the lattice, and thus we expect it to be correspondingly “gentle” with respect to its action on the lattice.

Indeed, as we show in Fig. 6(a), we do not see the lattices squeezed into sheets for the $m_z = +2$ mode. Instead we observe a gradual increase of disorder in the lattice. 400 msec after we start the excitation, we see a complete loss of long-range order in the vortex structure. The imaging contrast of individual vortices remains high, so we know they remain parallel to the line of sight (in contrast for instance to the case of Fig. 2), but otherwise they appear to have liquified (see the correlation histogram of Fig. 6). This behavior confirms our expectation of the $m_z = +2$ mode being a gentler disturbance for the lattice than the $m_z = -2$ mode.

Conclusions In conclusion we have succeeded in observing a wealth of nonequilibrium vortex lattice dynamics in a BEC under anisotropic compression. Key observations include the shifting of lattice planes relative to each other, leading to transient changes of the lattice structure, the formation of an unexpected and very pronounced sheet structure, and finally, a gradual transition from an ordered lattice to a rather liquid-like arrangement in which vortex cores remain visible, but their relative positions are irregular. The observed sheet structure is of particular interest: at present the behavior of densely packed vortex lattices is in the center of theoretical discussions about vortices [22–24]. While most of these theoretical discussions propose to enter this regime by having high rotation rates almost inaccessible to experiment or inconveniently low atom numbers in the condensate, this paper demonstrates an alternative and unexpected way of bringing vortices close together. We hope that the results presented in this Letter will stimulate further theoretical discussions in the field of vortex lattices.

The work presented in this paper was funded by NSF and NIST. PE acknowledges support by the Alexander von Humboldt Foundation.

* Quantum Physics Division, National Institute of Standards and Technology.

- [1] M. R. Matthews *et al.*, Phys. Rev. Lett. **83**, 2498 (1999); B. P. Anderson, P. C. Haljan, C. E. Wieman, and E. A. Cornell, Phys. Rev. Lett. **85**, 2857 (2000).
- [2] K.W. Madison, F. Chevy, W. Wohlleben, and J. Dalibard, Phys. Rev. Lett. **84**, 806 (2000).
- [3] K.W. Madison, F. Chevy, V. Bretin, and J. Dalibard, Phys. Rev. Lett. **86**, 4443 (2001).
- [4] J. R. Abo-Shaeer, C. Raman, J. M. Vogels, and W. Ketterle, Science **292**, 476 (2001).
- [5] P. C. Haljan, I. Coddington, P. Engels, and E. A. Cornell, Phys. Rev. Lett. **87**, 210403 (2001).
- [6] E. Hodby, G. Heckenblaikner, S.A. Hopkins, O.M. Maragó, and C. J. Foot, Phys. Rev. Lett. **88**, 010405 (2001).
- [7] D. A. Butts and D. S. Rokhsar, Nature **397**, 327 (1999).
- [8] C. Raman, J. R. Abo-Shaeer, J. M. Vogels, K. Xu, and W. Ketterle, Phys. Rev. Lett. **87**, 210402 (2001).
- [9] J. R. Abo-Shaeer, C. Raman, and W. Ketterle, Phys. Rev. Lett. **88**, 070409 (2002).
- [10] We impart angular momentum to the noncondensed cloud by stepwise driving a quarter cycle of a scissors mode [11].
- [11] O.M. Maragó, S.A. Hopkins, J. Arlt, E. Hodby, G. Heckenblaikner, and C.J. Foot, Phys. Rev. Lett. **84**, 2056 (2000).
- [12] B. P. Anderson, P. C. Haljan, C. A. Regal, D. L. Feder, L. A. Collins, C. W. Clark, and E. A. Cornell, Phys. Rev. Lett. **86**, 2926 (2001).
- [13] J. J. García-Ripoll and V. M. Pérez-García, Phys. Rev. A **64**, 053611 (2001).
- [14] D. L. Feder and C. W. Clark, Phys. Rev. Lett. **87**, 190401 (2001).
- [15] F. Chevy, K. W. Madison, and J. Dalibard, Phys. Rev. Lett. **85**, 2223 (2000).
- [16] P. C. Haljan, B. P. Anderson, I. Coddington, and E. A. Cornell, Phys. Rev. Lett. **86**, 2922 (2001).
- [17] F. Zambelli and S. Stringari, Phys. Rev. Lett. **81**, 1754 (1998).
- [18] S. Stringari, private communication. For an alternative approach, see also A. A. Svidzinsky and A. L. Fetter, Phys. Rev. A **58**, 3168 (1998).
- [19] We emphasize as well that the two different modes result in very different fluid-flow patterns. The $m_z = +2$ mode very closely approximates rigid-body rotation, while much of the $m_z = -2$ velocity field is provided by an irrotational, quadrupole flow pattern. This distinction may provide a parallel explanation for the correspondingly distinct observed effects.
- [20] We define ellipticity as $\frac{\omega_x^2 - \omega_y^2}{\omega_x^2 + \omega_y^2}$ with ω_x and ω_y being the trap frequency along the minor and major axes of the ellipse, respectively.
- [21] For related work on the evolution of the ellipticity see also P. Rosenbusch, D. S. Petrov, S. Sinha, F. Chevy,

V. Bretin, Y. Castin, G. Shlyapnikov, and J. Dalibard, con-mat/0201568.

[22] T. L. Ho, Phys. Rev. Lett. **87**, 060403 (2001).

[23] U. R. Fischer and G. Baym, condmat/0111443.

[24] B. Paredes, P. Zoller, and J. I. Cirac, condmat/0203061.

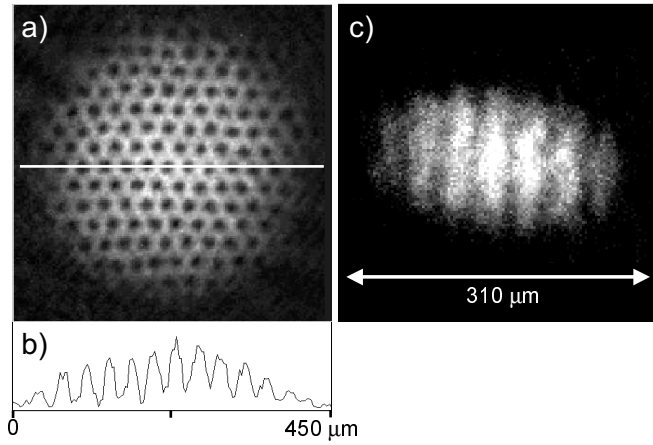


FIG. 1. (a) Expansion picture of a vortex lattice seen along the rotation axis. (b) One pixel wide cross section along the white line in (a). (c) Expansion picture of a different condensate rotating more slowly than in (a), seen from the side.

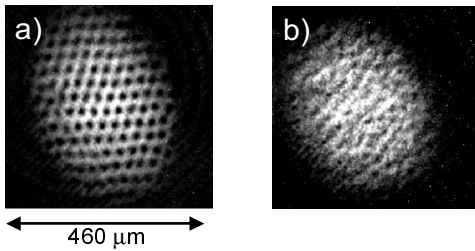


FIG. 2. Lattice evolution after an $m_z = -2$ excitation. Pictures taken (a) 173 ms and (b) 873 ms after start of trap deformation

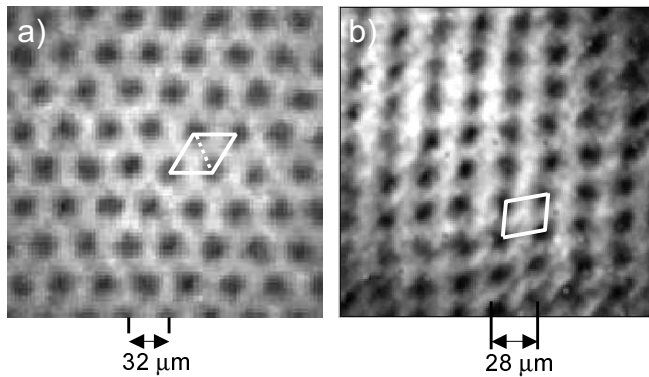


FIG. 3. Change of lattice structure. (a) Hexagonal structure in an undisturbed lattice. (b) Near orthorhombic structure seen transiently during lattice evolution in the presence of an $m_z = -2$ quadrupolar surface mode.

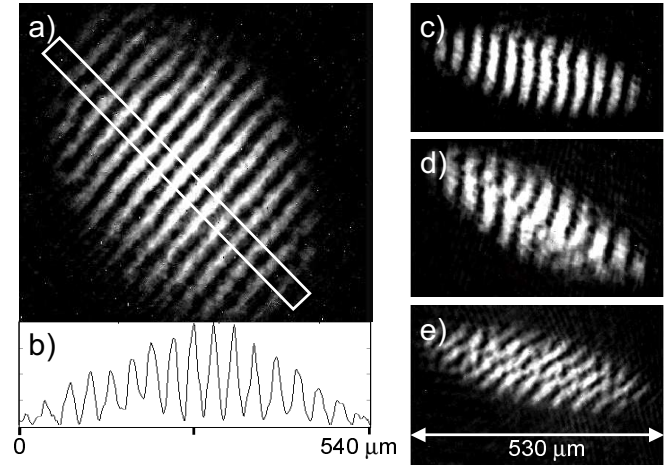


FIG. 4. (a) Sheet-like structure as seen during lattice evolution in the presence of an $m_z = -2$ quadrupolar surface mode. (b) Cross section integrated over the white box in (a). Even though the box is wider than the calculated vortex core spacing, the observed contrast is nearly perfect. (c-e) Same as (a), but observed in a more deformed trap with $\{\omega_{x,y,z}\} = 2\pi\{6.0, 8.6, 13.8\}$ Hz

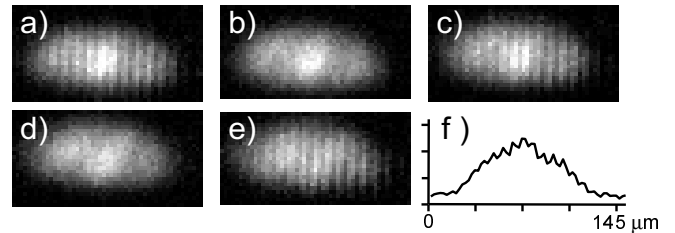


FIG. 5. (a-e) Nondestructive in-trap images of the sheet-like structures seen along the x-direction [conditions similar to Fig. 4(a)]. Spacing between images 10.6 ms. Note the very different spatial scale from expansion images (e.g., Fig. 1). (f) Cross section of (a), integrated over the condensate.

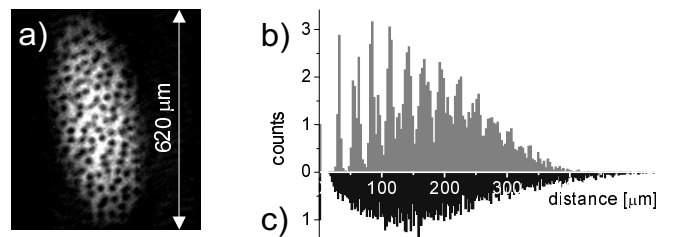


FIG. 6. (a) Irregular assembly of vortex cores as observed after 500 ms in the presence of an $m_z = +2$ quadrupolar surface mode. (b) Histogram of distances between each pair of vortices in the regular hexagonal lattice shown in Fig. 1a. The visibility of separate peaks reveals the high degree of long-range order. (c) Same as (b) but calculated for the BEC of Fig. 6a. Peaks are barely visible here, meaning that the lattice has almost reached a random disorder.